Vol. 746: 17–33, 2024
https://doi.org/10.3354/meps14682

MARINE ECOLOGY PROGRESS SERIES
Mar Ecol Prog Ser

Published October 8

Isolation and characterization of plant growth-promoting rhizobacteria (PGPR) from eelgrass *Zostera marina* rhizosphere: implications for bioremediation

Jie Sun[1,2], Yan-Hao Zhang[1,2], Xiang Zhao[1,2], Wen-Jie Yan[1,2], Wen-Tao Li[1,2], Pei-Dong Zhang[1,2,*]

[1]Key Laboratory of Mariculture (Ocean University of China), Ministry of Education, Qingdao 266003, PR China
[2]Joint Research Center for Conservation, Restoration & Sustainable Utilization of Marine Ecology, Ocean University of China–China State Shipbuilding Corporation Environmental Development Co., Ltd., Qingdao 266100, PR China

ABSTRACT: Plant growth-promoting rhizobacteria (PGPR) play a crucial role in enhancing plant growth. However, investigations into the presence and function of PGPR in seagrass rhizospheres remain relatively limited. In this study, we isolated 45 strains of PGPR from *Zostera marina* rhizospheres and assessed their functional attributes. Additionally, we evaluated the performance of these candidate strains under varying environmental conditions, such as temperature, salinity, and pH. Out of the 45 analyzed strains, 6 were found to possess the *nif*H gene; some strains also exhibited the ability to solubilize inorganic phosphorus, with dissolved phosphorus content ranging widely from 14.6 to 393.9 mg l^{-1}. Eleven strains demonstrated indole-3-acetic acid production, with yields spanning from 16.3 to 42.8 mg l^{-1}. Siderophores and ammoniated proteins were produced by 32 and 20 strains, respectively. Notably, 5 PGPR strains (F65, G84, G85, G86, and I109) displayed multiple growth-promoting properties along with strong adaptability to a wide range of physicochemical conditions. This study highlights the potential reservoir of PGPR in the eelgrass rhizosphere and provides significant implications for utilizing these bacteria to enhance the success rate of restoring degraded seagrass meadows.

KEY WORDS: PGPR · *Zostera marina* · Seagrass restoration · Growth-promoting properties · Culture conditions

1. INTRODUCTION

Seagrasses, as foundational species in coastal ecosystems, exhibit high primary productivity (Harborne et al. 2006, Short et al. 2007, McKenzie et al. 2020). Seagrass meadows offer numerous ecological and economic benefits, including improving water clarity, serving as crucial nursery habitats for diverse marine species, mitigating shoreline erosion by dissipating wave energy, reducing exposure to bacterial pathogens of humans, and playing a pivotal role in nutrient cycling and carbon sequestration (Duarte & Chiscano 1999, Moore 2009, Duarte et al. 2010, Lamb et al. 2017, James et al. 2019, Unsworth et al. 2019). However, they are experiencing significant degradation primarily due to persistent anthropogenic pressures such as aquaculture and land-based pollutants (Dunic et al. 2021). Recent research has revealed alarming statistics indicating that approximately 19.1% of seagrass meadows worldwide have experienced deterioration since 1880 (Dunic et al. 2021), with localized declines reaching levels as high as

*Corresponding author: zhangpdsg@ouc.edu.cn

40–90% (Zheng et al. 2013, Fraser & Kendrick 2017, Leblanc et al. 2023).

Seagrass transplantation, a commonly employed restoration strategy, aims to address the decline of seagrass meadows (Orth et al. 1999, Tan et al. 2020). However, a global meta-analysis of seagrass restoration trials revealed that the average success rate for restoration was only 37% (van Katwijk et al. 2016). Several influential factors have been identified as crucial elements affecting the success of restoration projects, including site selection, methodologies for collection and planting, timing of transplants, and the impact of bioturbation by resident fauna within restored meadows (van Katwijk et al. 2009, Zhang et al. 2014). Despite the increasing attention devoted to the impact of sedimentary microbial communities on seagrass growth and survival in recent years (Tan et al. 2020, Mohr et al. 2021, Szitenberg et al. 2022), there remains a research gap concerning the identification of bacteria with potential for restoring degraded meadows.

The concept of plant growth-promoting rhizobacteria (PGPR) was introduced by Kloepper & Schroth (1978) to characterize soil bacteria that are free-living, thrive within the rhizosphere, and exhibit vigorous root colonization, ultimately promoting plant growth. Several studies have demonstrated the potential of specific bacterial communities in sediments to promote seagrass recovery (Hansen et al. 2000, Milbrandt et al. 2008, Celdrán et al. 2012, Cole & McGlathery 2012, Rabbani et al. 2021). For example, the nitrogen fixed by *Azotobacter* has the potential to satisfy up to 20–90% of nitrogen requirements for eelgrass growth (Hansen et al. 2000, Cole & McGlathery 2012). However, transplantation activities often disrupt the rhizosphere populations of PGPR, leading to insufficient colonization around seagrass transplants. The strains involved in the nitrogen, phosphorus, and iron cycles can supplement the nutrient requirements of transplanted plants. Furthermore, understanding the optimal growth conditions of these bacteria will facilitate their large-scale fermentation for formulation into microbial inoculants. Therefore, an approach involving isolation of PGPR from their natural habitats followed by population propagation through fermentation and formulation is necessary for successful large-scale seagrass restoration efforts. This approach effectively mitigates transplantation shock caused by disrupted rhizosphere bacterial communities and enhances the survival and growth of seagrass transplants (Bender et al. 2016, Naamala & Smith 2020, Rabbani et al. 2021, Vogel et al. 2021, Wang et al. 2021).

Zostera marina, a dominant eelgrass species in temperate regions of the northern hemisphere, has emerged as a primary focus for restoration endeavors due to ongoing habitat losses (Zhang et al. 2020, 2022). In this study, we isolated and identified potential PGPR strains from *Z. marina* rhizospheres using field sampling and sequencing techniques. Subsequently, we assessed their functional characteristics and optimized their culture conditions through single-factor and response surface experiments. The objectives of this research were to evaluate the growth-promoting properties of PGPR strains derived from *Z. marina* rhizospheres and determine their optimal culture conditions. This study highlights *Z. marina* rhizospheres as a valuable source of culturable bacteria with growth-promoting attributes, unveiling the potential use of PGPR in restoring degraded seagrass meadows and providing a foundation for future restoration strategies.

2. MATERIALS AND METHODS

2.1. Sample collection

Eelgrass plants were aseptically collected with a sterile shovel from a 50 × 50 m donor bed located in a *Zostera marina* meadow in Swan Lake (37° 21′ N, 122° 34′ E), Rongcheng, Shandong Province, China, in October 2021 (Fig. 1). The loosely attached soil surrounding the roots was gently removed to collect rhizosphere samples within approximately 1–3 mm from the root (Zhuang et al. 2021, Jiang et al. 2023). All collected samples were immediately placed in sterilized polyethylene bags, stored at 4°C, and transported to the laboratory within 4 h. At the same time, temperature (mercury thermometer), salinity (YSI 650 MDS), and pH (PHS-25) in seawater, and available nitrogen, available phosphorus, sulfide, and petroleum hydrocarbons (C_{10}–C_{40}) in sediments were measured (±SD) as 23 ± 1.0°C; 27.7± 0.4 PSU; 8.1± 0.5; and 13.6 ± 2.2, 4.24 ± 0.3, 52.3 ± 5.7, and 26.0 ± 2.7 mg kg^{-1}, respectively.

2.2. Experimental procedure and sample calculations

2.2.1. Isolation of root-associated bacteria

In the laboratory, a total of 10 g of rhizosphere soils was aseptically transferred into a sterile 250 ml conical bottle containing 90 ml of sterile saline solution (0.85% NaCl) and was shaken (180 rpm for 30 min) at 28°C to form a sediment suspension. The suspension

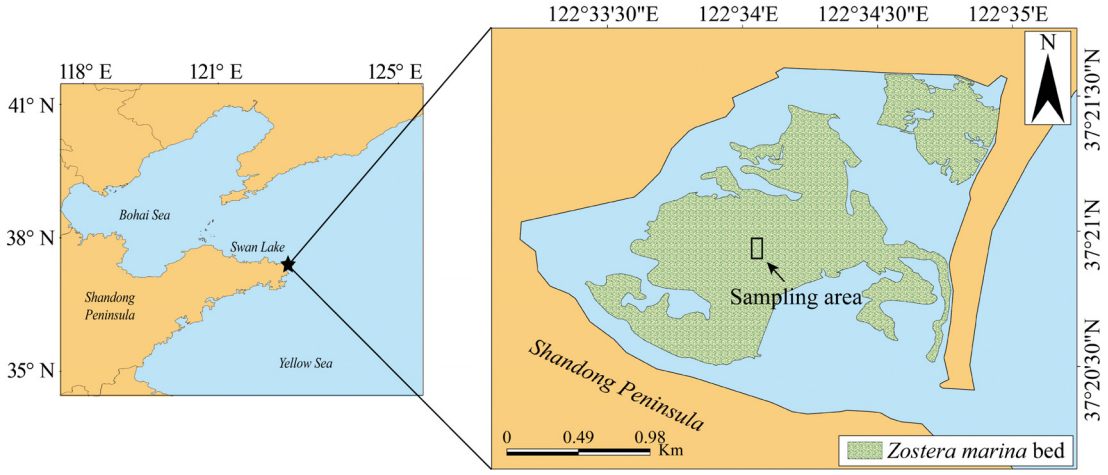

Fig. 1. Swan Lake, Shandong Province, China, showing location of the sampling area

was serially diluted into concentration gradients of 10^{-2}, 10^{-3}, 10^{-4}, 10^{-5}, and 10^{-6}. Then, 0.1 ml of each dilution with 3 replicates was evenly spread onto 2216E medium (Wang et al. 2015), National Botanical Research Institute phosphate (NBRIP) medium (Li et al. 2019), and Ashby's nitrogen-free selective medium (Wakarera et al. 2022), respectively. The 2216E medium provides an optimal environment for the proliferation of diverse aquatic microorganisms and is extensively utilized in marine microbiology research. The NBRIP medium is employed for the screening of phosphate-solubilizing bacteria, while Ashby's medium serves as a selective culture medium specifically designed for the isolation and cultivation of autotrophic nitrogen-fixing bacteria. Plates were incubated at 28°C for 2–7 d. Colonies exhibiting distinct morphologies were carefully selected for further purification on 2216E culture medium and incubated for an additional 24–48 h at 28°C. The purified isolates were then preserved in 20% glycerol at −80°C until further use.

2.2.2. Genotypic characterization of bacterial isolates

The taxonomic classification of purified strains, which exhibited distinct morphological differences, was determined using the 16S rRNA technique. DNA extraction was conducted using the Bacterial DNA Isolation Kit (Norgen Biotek). The 16S rRNA genes of the isolated colonies were amplified using a 30 µl PCR mixture as follows: 15 µl of *Taq* polymerase PCR Mix (Takara), 13 µl of double distilled water (dd water), 1 µl of template DNA, and 0.5 µl each of forward oligonucleotide primer 27F (5′-AGA GTT TGA TCA TGG CTC AG-3′) and reverse primer 1492R (5′-GTT TAC CTT GTT ACG ACT T-3′). The PCR conditions comprised an initial denaturation step at 94°C for 5 min; followed by 30 cycles of denaturation at 94°C for 1 min, annealing at 55°C for 1 min, extension at 72°C for 1.5 min; and a final extension step at 72°C for 10 min. The PCR products were subsequently sent to BGI Genomics (Shenzhen) for sequencing analysis. The obtained sequences were analyzed using the Blast-N program available through the NCBI web service (www.ncbi.nlm.nih.gov/) (Altschul et al. 1990).

2.3. Screening of root-associated bacteria as potential PGPR

2.3.1. Growth in nitrogen-free medium and *nif*H gene amplification

The *nif*H gene serves as the most extensively sequenced marker gene utilized for the identification of nitrogen-fixing bacteria. According to the conditions described by Gaby & Buckley (2012), the *nif*H gene fragment (360 bp), encoding nitrozyme reductase, was PCR-amplified from strains capable of growing on Ashby's nitrogen-free selected medium using the primers *nif*HF (5′-ATG TCG GYT GYG AYC CSA ARG C-3′) and *nif*HR (5′-ATG GTG TTG GCG GCR TAV AKS GCC ATC AT-3′). The PCR conditions comprised an initial denaturation step at 94°C for 5 min; followed by 30 cycles of denaturation at 94°C for 30 s, annealing at 55°C for 30 s, extension at 72°C for 30 s; and a final extension step at 72°C for 10 min.

2.3.2. Phosphate solubilization

For qualitative determination, the strains that could grow on the NBRIP medium during the initial screening were spotted onto the NBRIP medium with sterilized

toothpicks according to the method of Nautiyal (1999). Each strain was spotted 3 times. Subsequently, the petri dishes were incubated at 28°C for 5 d to observe the presence of clear halos (halozones) around the colonies. To assess phosphate solubilization, the phosphate solubilization index (PSI) was determined for colonies surrounded by clear halos according to the method reported by Serrano et al. (2013): PSI = (colony diameter + halozone diameter) / colony diameter.

For quantitative determination, overnight activation was performed on strains that produced clear halos and on strains that grew well on NBRIP medium although they did not produce clear halos. Subsequently, a 1% inoculum size of these activated cultures was transferred to NBRIP liquid medium and incubated at 28°C with agitating at 180 rpm for 5 d. Each strain was tested 3 times. The concentration of dissolved phosphorus was measured by subjecting the supernatant from a 1 ml bacterial suspension (obtained through centrifugation at 4000 rpm (1400 × *g*) for 30 min) to quantification using the antimony molybdenum colorimetric method described by Houida et al. (2022). The pH measurements of the liquid medium were conducted both at the beginning and end of the experiment.

2.3.3. Production of indole-3-acetic acid (IAA)

For qualitative determination, the IAA production test was performed with all 45 strains determined after sequencing, and repeated 3 times for each strain. Each isolate was inoculated into 2216E medium supplemented with L-tryptophan (200 g ml^{-1}) and incubated at 28°C with agitation (180 rpm for 48 h) to assess the IAA production capability. Subsequently, 50 µl of bacterial suspension were dispensed into individual wells of a 96-well plate. Salkowski chromogenic reagent (consisting of 1 ml 0.5 mol l^{-1} $FeCl_3$ and 50 ml 35% $HClO_4$) was added twice to the bacterial suspension, following the method described by Bric et al. (1991). An IAA standard solution (50 mg l^{-1}) was used as a positive control, while uninoculated medium served as the negative control. The 96-well plate was then placed in darkness at 25°C for 30 min. The development of a pink color indicated the capacity of the strain to produce IAA.

The quantitative assessment of IAA yield was performed on strains that exhibited positive results (pink) in the qualitative experiment, and repeated 3 times for each strain. A 1.5 ml bacterial suspension was collected into a 2 ml centrifuge tube and subjected to centrifugation at 10 000 rpm (9000 × *g*) for 15 min. Subsequently, 1 ml of the supernatant was mixed with 2 ml of Salkowski's solution, and the mixture was kept in darkness for 30 min. The absorbance of the solution was determined at 530 nm using a spectrophotometer and quantified by referencing a standard curve that was prepared separately using known concentrations of commercial IAA (Sigma-Aldrich) (Houida et al. 2022).

2.3.4. Production of siderophores

The siderophore production test was performed with all 45 strains determined after sequencing, and repeated 3 times for each strain. Siderophore production was assessed using petri dishes containing catechol amphiphilic substances (CAS)-agar, with the composition of the CAS blue solution following the specifications reported by Schwyn & Neilands (1987). Pure isolates were aseptically inoculated onto CAS agar plates using sterile toothpicks and then incubated at 28°C for a period of 7–10 d. Colonies exhibiting orange zones around them were identified as siderophore-producing strains. To assess the siderophore production capacity, the solubilization index (SI) was determined according to the presence of an orange halo around the colony as: SI = (colony diameter + halozone diameter) / colony diameter.

2.3.5. Production of NH_3

The NH_3 production test was performed with all 45 strains determined after sequencing. The strains were inoculated into test tubes containing a peptone solution (10 g l^{-1}) and incubated at 28°C with agitation (180 rpm for 72 h). After incubation, 0.5 ml of Nessler's reagent was added to each tube, and uninoculated medium served as the control. The appearance of a yellow color upon the addition of Nessler's reagent indicated the presence of accumulated ammonia, following the method described by Singh et al. (2020).

2.4. Optimization of strain culture conditions

Understanding the optimal growth conditions for bacteria in liquid media is crucial for enhancing the biomass production of specific strains, given the varied factors influencing bacterial proliferation. This is particularly significant in studies of bacteria, where strains often have distinct environmental requirements and some may exhibit slow and particular growth patterns. A series of single-factor experiments on tem-

perature, salinity, and pH were conducted to optimize the culture conditions for strains selected with at least 4 growth-promoting characteristics. Each single-factor experiment was maintained for 48 h and repeated 3 times. The optical density at 600 nm (OD_{600}) of each treatment was measured using an ultra-sensitive microplate reader workstation (SpectraMax i3x). The culture temperature, the salinity of the liquid culture medium, and the pH were optimized along with their interactions by using a Box-Behnken design of response surface methodology.

2.4.1. Temperature optimization

The experiment consisted of 8 temperature treatments (16, 20, 24, 28, 32, 36, 40, and 44°C). The activated bacterial solution was inoculated into a 2216E liquid medium (pH = 7.2, salinity = 30 PSU) using 1% inoculum size. The samples were incubated in a shaking incubator (180 rpm for 48 h) under different temperature treatments. Subsequently, OD_{600} was measured to assess the growth and reproduction of the strains.

2.4.2. Salinity optimization

The experiment consisted of 7 salinity treatments (10, 15, 20, 25, 30, 35, and 40 PSU). The activated bacterial solution was inoculated into a 2216E liquid medium (pH = 7.2) using 1% inoculum size. The samples were incubated at 28°C in a shaking incubator (180 rpm for 48 h) under different salinity treatments. Subsequently, OD_{600} was measured to assess the growth and reproduction of the strains.

2.4.3. pH optimization

The experiment consisted of 8 pH treatments (3.0, 4.0, 5.0, 6.0, 7.0, 8.0, 9.0, and 10.0). The activated bacterial solution was inoculated in a 2216E liquid medium (salinity = 30 PSU) using 1% inoculum size. The samples were incubated at 28°C in a shaking incubator (180 rpm for 48 h) under different pH treatments. Subsequently, OD_{600} was measured to assess the growth and reproduction of the strains.

2.4.4. Response surface methodology

A Box-Behnken design was employed to optimize the interactions among temperature, salinity, and pH of the culture liquid medium using the statistical software Design Expert 13 (StatEase). The *F*-value was computed through analysis of variance to establish the most appropriate model for data fitting (Tables S1—S5 in the Supplement at www.int-res.com/articles/suppl/m746p017_supp.pdf). The mathematical relationship between the response variable (Y, OD_{600}) and the independent variables (X_i) was modeled by a second-order polynomial function:

$$Y = \beta_0 + \beta_1 X_1 + \beta_2 X_2 + \beta_3 X_3 + \beta_{11} X_1^2 + \beta_{22} X_2^2 + \beta_{33} X_3^2 + \beta_{12} X_1 X_2 + \beta_{13} X_1 X_3 + \beta_{23} X_2 X_3 \quad (1)$$

where Y: predicted response (OD_{600}); β_0: intercept; β_1, β_2, and β_3: linear coefficients; β_{11}, β_{22}, and β_{33}: squared coefficients; β_{12}, β_{13} and β_{14}: interaction coefficients of the equation; X_1, X_2, and X_3: independent variables, representing temperature, salinity, and pH, respectively. The optimal fermentation conditions identified by the Box-Behnken design were validated by conducting 3 parallel experiments, thus ensuring the scientific rigor and reliability of the experimental model.

2.5. Statistical analysis

The data are reported as means ± SD. Bar charts and 3D response surface maps were generated using OriginPro 2022b software (OriginLab). A phylogenetic tree was constructed using the neighbor-joining method in MEGA 6.0. In response surface experiments, the significance of the effect of the independent variables on the response was assessed using ANOVA and Fisher's test, with $p < 0.05$ indicating significance. The multiple correlation coefficient (R^2) and adjusted R^2 were utilized as quality indicators for evaluating the fit of the second-order polynomial model equation.

3. RESULTS

3.1. Isolation and identification of PGPR

A total of 45 bacterial strains were isolated and identified using field sampling and sequencing techniques (Table S6). The results of 16S rRNA gene sequencing revealed that the bacterial isolates belonged to 4 phyla, 6 classes, and 41 genera. *Pseudomonadota* accounted for the majority at 71.1%, followed by *Bacilli* at 17.8%, *Bacteroidota* at 6.7%, and *Actinobacteriota* at 4.4% (Fig. 2). The sequences obtained in this study were uploaded and are available in GenBank under accession number SUB14420082.

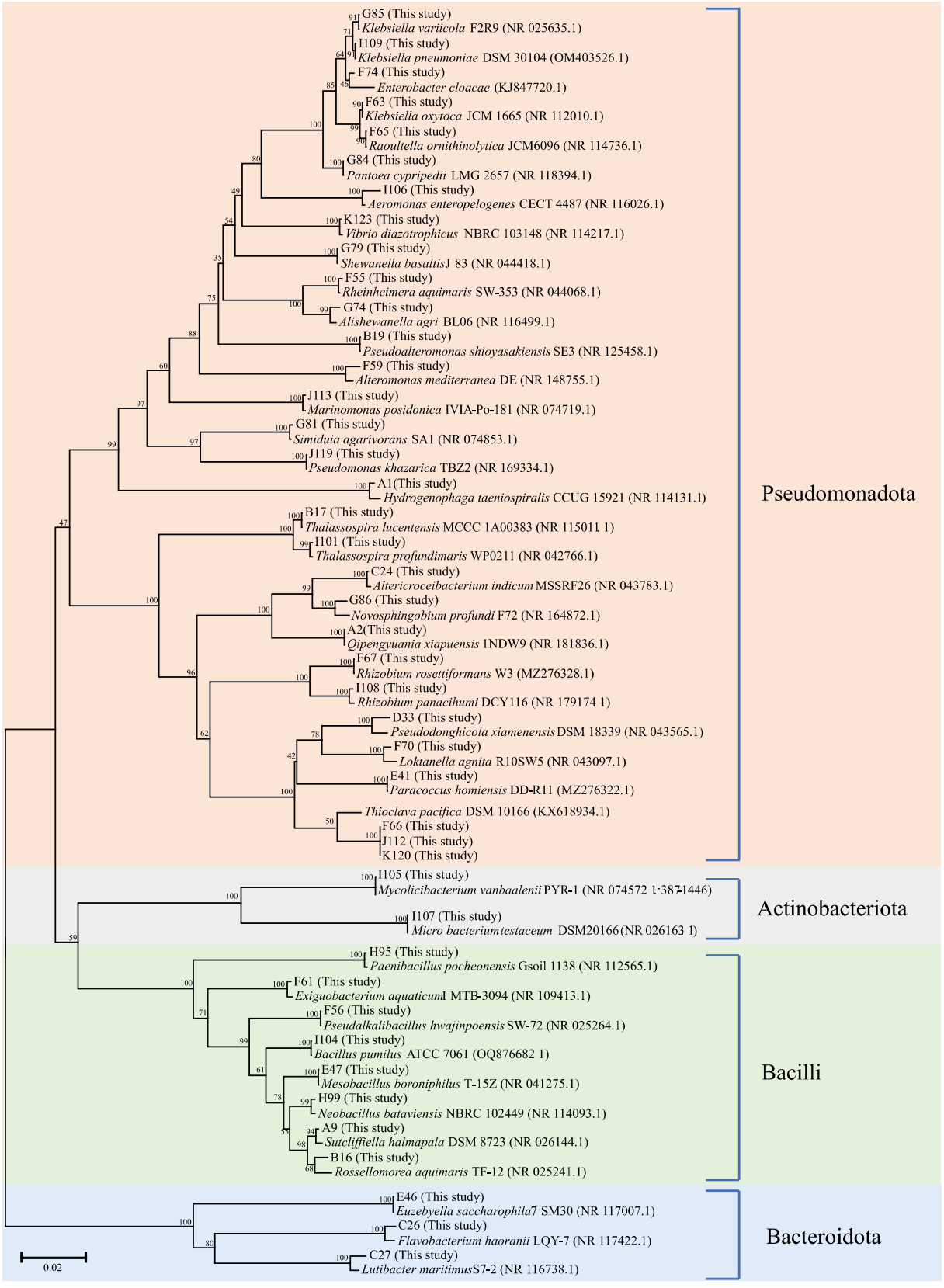

Fig. 2. Distribution and abundance of bacteria isolated from the *Zostera marina* rhizosphere

3.2. Screening of root-associated bacteria as potential PGPR

3.2.1. Nitrogen fixation

Six strains (F63, G79, G84, G85, G86, and J111) were amplified for the *nif*H gene, producing a 360 bp product (Fig. 3). Molecular analysis based on 16S rRNA gene sequencing revealed that these 6 isolates exhibited maximum sequence similarity to *Klebsiella oxytoca* JCM 1665 (99.58%), *Shewanella basaltis* J83 (99.65%), *Pantoea cypripedii* LMG 2657 (98.66%), *K. variicola* F2R9 (99.86%), *Novosphingobium profundi* F72 (98.83%), and *Gallaecimonas pentaromativorans* CEE 131 (99.65%), respectively.

3.2.2. Phosphate solubilization

Six strains (F65, G71, G84, G85, I109, and K123) exhibited halozones on Pikovskaya's agar (NBRIP medium + agar), while strains G86 and J120 displayed normal growth on the medium but lacked halozones (Fig. 4). The PSI of the isolates ranged from 2.1 to 7.0 (Table 1). Quantitative experiments revealed that strain J120 demonstrated the highest phosphorus dissolution ability, with a dissolved amount of up to 393.9 mg l^{-1}. Strain G84 exhibited limited ability, with only 14.6 mg l^{-1} dissolved amount. The remaining strains released soluble orthophosphate in the range of 28.8 mg l^{-1} to 130.5 mg l^{-1}. The pH of the medium decreased within a range of 5.4 to 6.7. Pearson correlation analysis revealed a significant negative correlation between the pH of the culture medium and phosphorus solubilization by the strains ($p < 0.001$); however, no significant correlation was observed with PSI ($p = 0.510$) (Table 2).

3.2.3. Production of IAA

Among the 45 tested strains, 11 exhibited the ability to produce IAA (Fig. 5A). Quantitative analysis revealed that strain I109 displayed the highest level of IAA production (42.8 mg l^{-1}), while the remaining strains produced IAA within a range of 16.3–34.9 mg l^{-1} (Fig. 5B).

3.2.4. Production of siderophores

The isolates obtained in this study also demonstrated promising results with regard to siderophore production. Out of the 45 isolates obtained, 32 (72.7%) were capable of producing siderophores. However, a few strains exhibited low solubility indices, with only 12 strains surpassing a solubility index of 2.5 (Fig. 6A). Among them, strain E46 displayed the highest solubility index (4.05 ± 0.29), while strain F67 exhibited the lowest solubility index (2.90 ± 0.40) (Fig. 6B).

3.2.5. Production of NH_3

In an *in vitro* examination to detect ammonia production, positive results were observed in 20 strains (44.4%) (Fig. 7). Notably, strains C26, F63, F65, F66, G86, I104, I106, and J112 exhibited significant color changes compared to the control, indicating their ability to produce ammonia.

3.3. Strain culture conditions

3.3.1. Strain F65

The OD_{600} of strain F65 initially increased with the elevation in culture temperature, reaching a

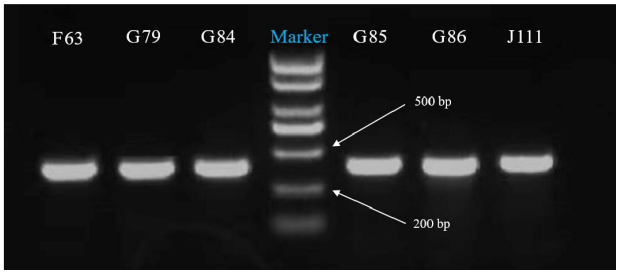

Fig. 3. PCR amplification of the *nif*H gene from genomic DNA of 6 bacterial strains isolated from the *Zostera marina* rhizosphere

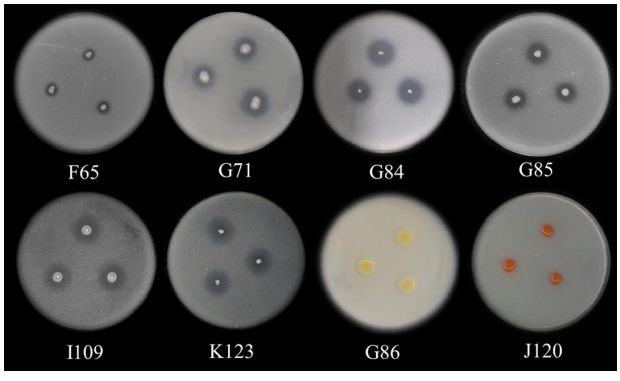

Fig. 4. Assessment of the phosphate-solubilization ability of bacterial strains isolated from the *Zostera marina* rhizosphere. Strains G86 and J120 show normal growth and lack halozones; the other 6 strains display halozones

Table 1. Comparison of tricalcium phosphate solubilization by bacterial isolate strains in agar and broth using NBRIP medium. Data are expressed as means ± SD. PSI: phosphate solubilization index

Strain	PSI	Broth (mg l^{-1} P solubilized)	pH of medium
F65	2.1 ± 0.2	75.9 ± 1.8	5.9 ± 0.1
G71	2.6 ± 0.2	130.5 ± 8.1	5.8 ± 0.3
G84	7.0 ± 0.9	14.6 ± 0.8	6.7 ± 0.1
G85	5.7 ± 0.9	64.6 ± 10.1	6.0 ± 0.2
G86	–	96.4 ± 1.0	6.1 ± 0.4
I109	3.6 ± 0.4	28.8 ± 2.4	6.2 ± 0.0
J120	–	393.9 ± 45.2	5.4 ± 0.1
K123	6.6 ± 0.5	107.2 ± 9.2	5.9 ± 0.3

Table 2. Pearson correlation analysis between phosphate solubilization index (PSI), broth (P solubilized), and pH of the medium. ** indicates a highly significant correlation between the 2 indicators ($p < 0.01$)

	PSI	Broth (mg l^{-1} P solubilized)	pH of medium
PSI	1		
Broth (mg l^{-1} P solubilized)	0.152	1	
pH of medium	−0.354	−0.824**	1

maximum value of 0.623 at 36°C, followed by a sharp decline to 0.074 at 44°C (Fig. 8A). Salinity levels ranging from 10 to 40 PSU exhibited a negligible impact on the proliferation of the strain (Fig. 8B). The highest OD_{600} value of 0.581 was observed at 20 PSU, while the lowest value of 0.480 was recorded at 40 PSU. Strain F65 demonstrated a preference for weak acidic conditions over alkaline environments (Fig. 8C). The regression model describing the relationship between the OD_{600} value of strain F65 and the factors influencing the growth is as follows:

$$OD_{600} = -18.61 + 0.67X_1 + 1.80X_2 + 2.71X_3 - 0.01X_1X_2 - 0.01X_1X_3 + 0.02X_2X_3 - 0.01X_1^2 - 0.42X_2^2 - 0.25X_3^2 \quad (2)$$

Based on model predictions, the ideal fermentation parameters were determined to be a culture temperature of 33.607°C, salinity of 20.810 PSU, and pH of 4.564, resulting in a predicted OD_{600} value of 0.660 (Fig. 8D–F). For experimental convenience purposes, the strain was fermented at a temperature of 34°C, salinity of 21 PSU, and pH of 4.5 for 3 repeated experiments conducted over a period of 48 h each time. The average obtained OD_{600} value of 0.636 was approximately equal to that predicted by the model.

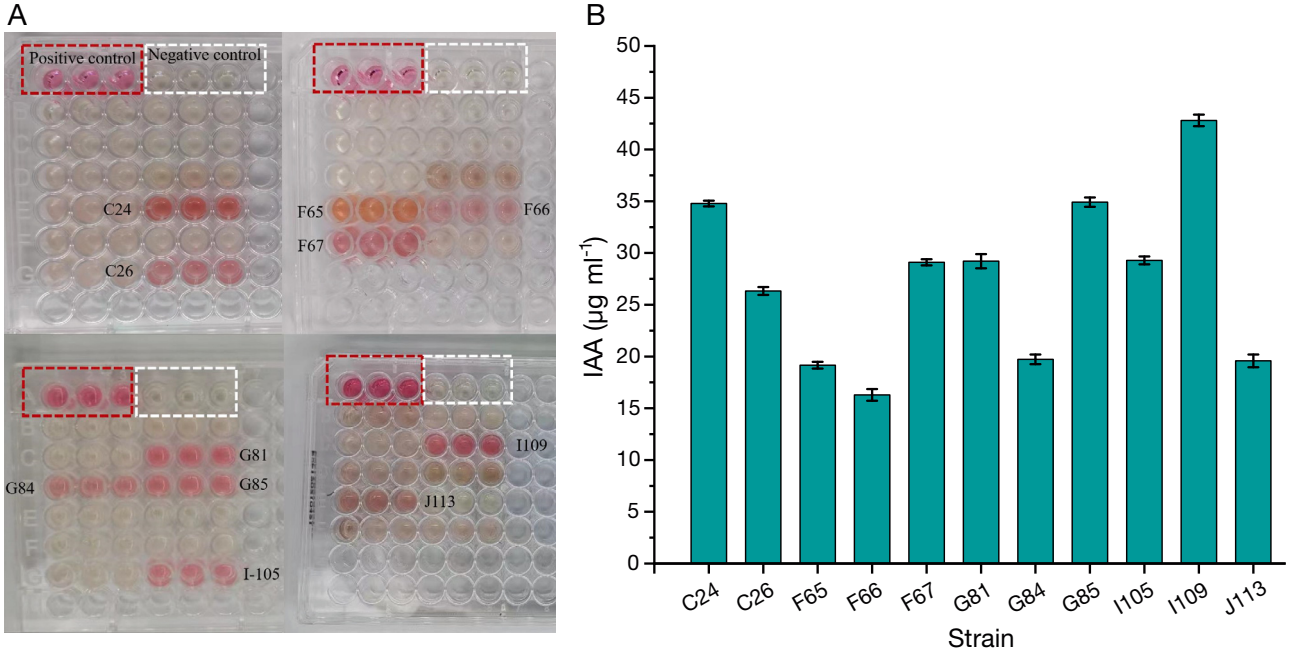

Fig. 5. Determination of the indole-3-acetic acid (IAA)-production ability of bacterial strains isolated from the *Zostera marina* rhizosphere. (A) Visualization of IAA through a color reaction; the 11 strains that exhibited an ability to produce IAA are labeled. (B) Quantification of the IAA-production ability of each of the 11 strains

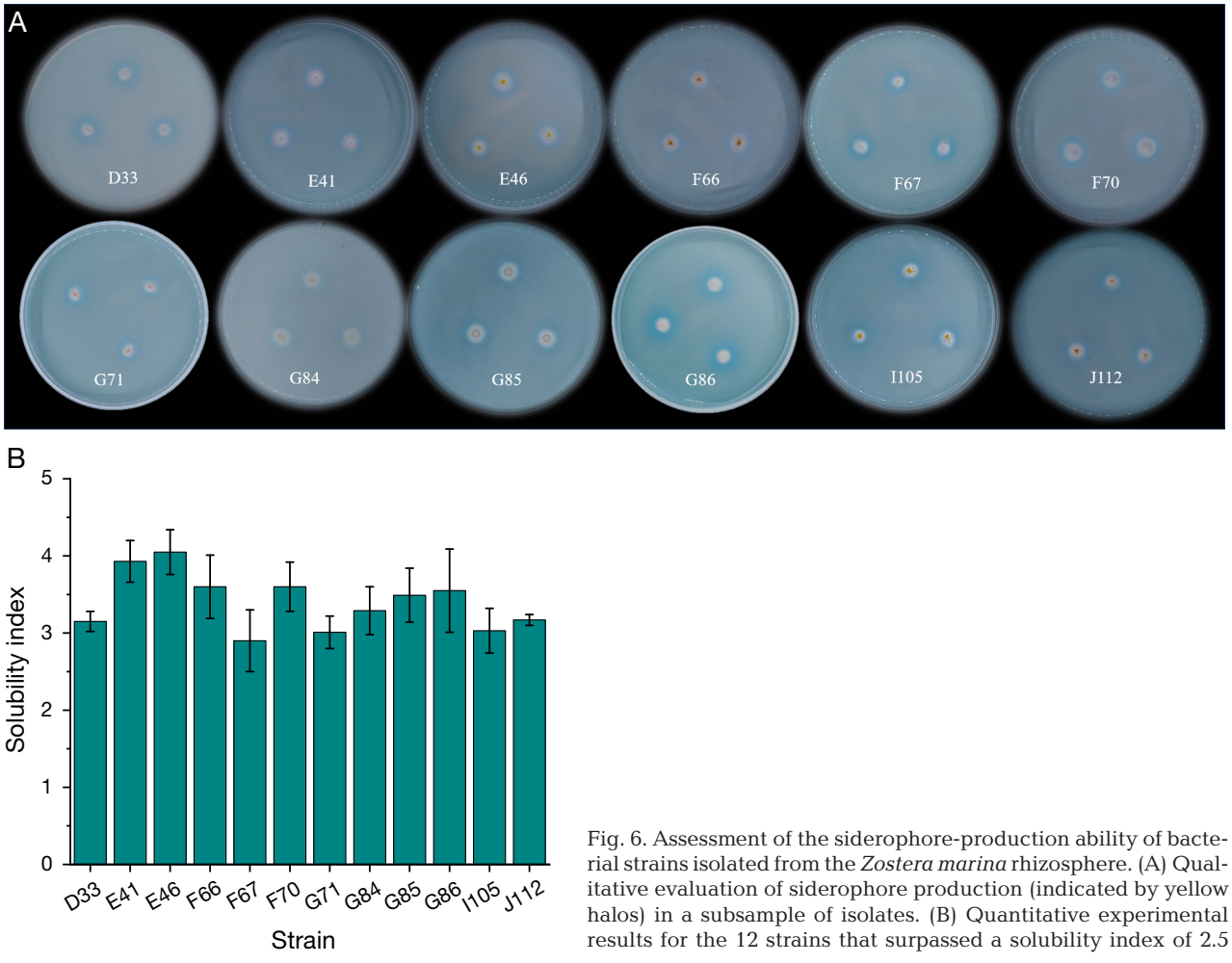

Fig. 6. Assessment of the siderophore-production ability of bacterial strains isolated from the *Zostera marina* rhizosphere. (A) Qualitative evaluation of siderophore production (indicated by yellow halos) in a subsample of isolates. (B) Quantitative experimental results for the 12 strains that surpassed a solubility index of 2.5

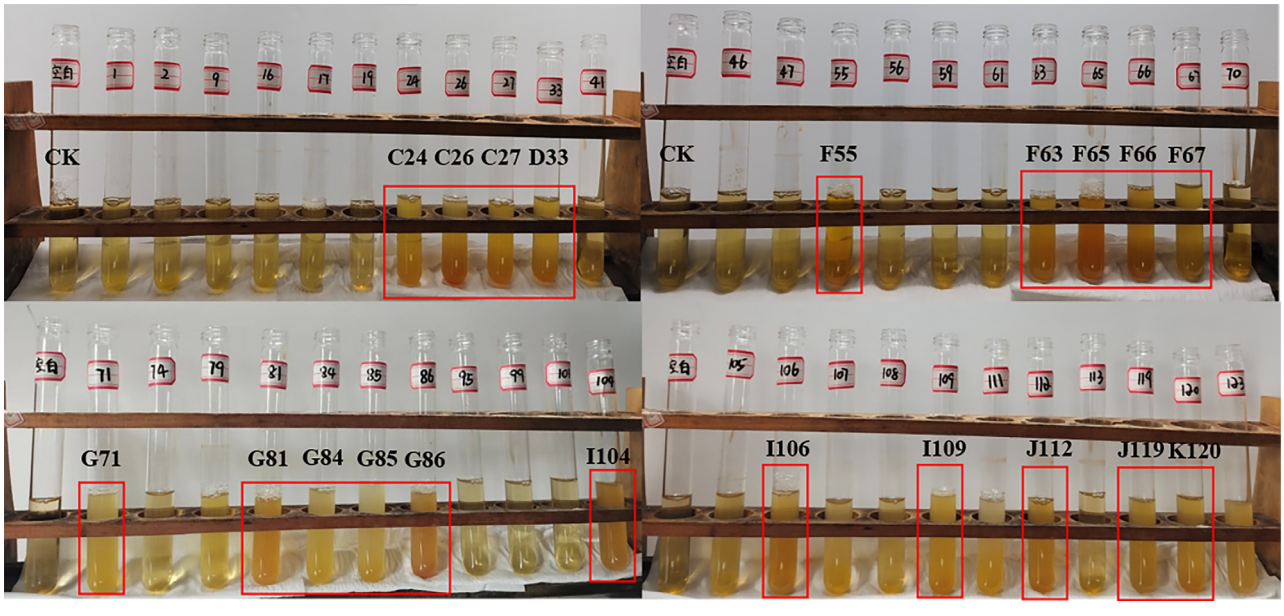

Fig. 7. Assessment of the ammonia-production ability of bacterial strains isolated from the *Zostera marina* rhizosphere. Strains surrounded by red boxes showed color changes compared to the control, indicating their ability to produce ammonia

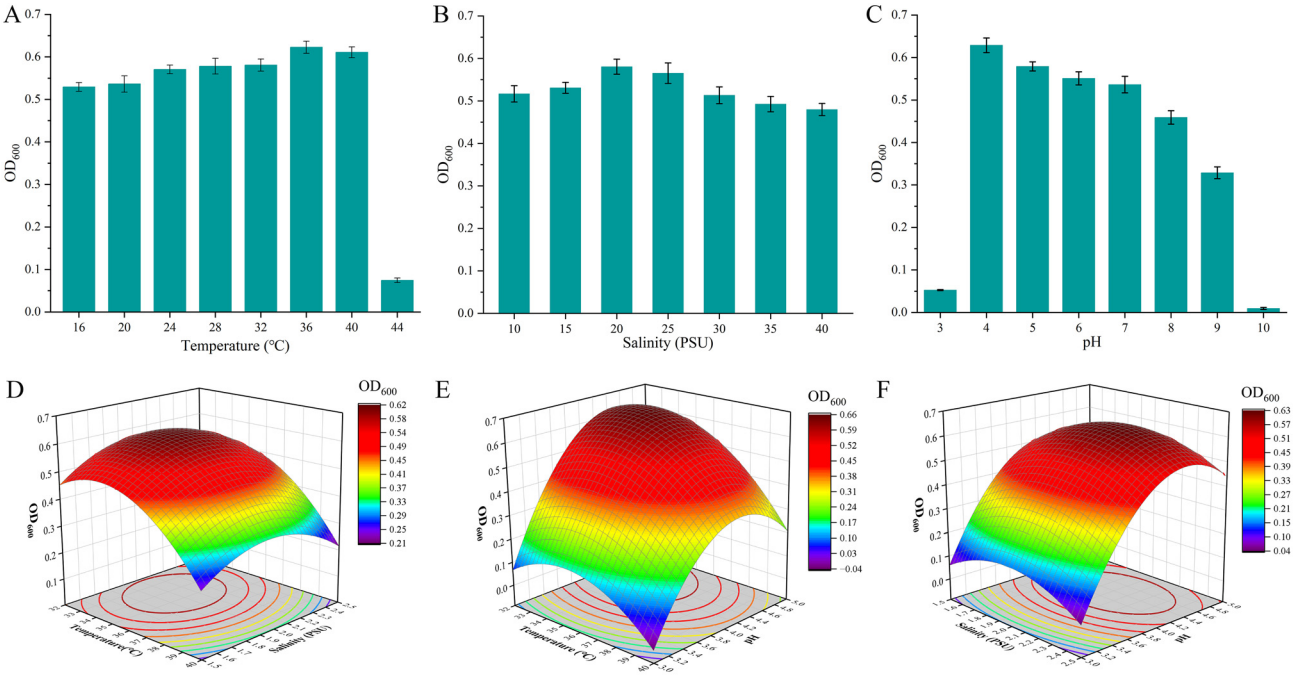

Fig. 8. Effect of cross-interaction among (A) culture temperature, (B) salinity, and (C) pH on the optical density at 600 nm (OD_{600}) of bacterial strain F65 isolated from the *Zostera marina* rhizosphere. (D–F) Combined effect of (D) temperature and salinity, (E) temperature and pH, and (F) pH and salinity. Data are expressed as means ± SD

3.3.2. Strain G84

The OD_{600} of strain G84 initially increased with the elevation in culture temperature, reaching a maximum value of 0.616 at 24°C, followed by a decline to 0.042 at 44°C (Fig. 9A). The effect of salinity on strain G84 was similar to that observed for strain F65, with the highest OD_{600} value (0.532) recorded at 20 PSU, while the lowest value (0.354) was observed at 40 PSU (Fig. 9B). Strain G84 exhibited an increasing trend in OD_{600} values, peaking at pH 6.0 (0.543), and subsequently decreasing to a minimum value of 0.001 at pH 10.0 (Fig. 9C). The regression model describing the relationship between the OD_{600} value of strain G84 and its growth-influencing factors is as follows:

$$OD_{600} = -4.21 + 0.26X_1 + 0.55X_2 + 0.37X_3 - 0.01X_1X_2 + 0.01X_1X_3 - 0.01X_2X_3 - 0.01X_1^2 - 0.07X_2^2 - 0.04X_3^2 \quad (3)$$

The optimal fermentation parameters were determined based on model predictions, which included a culture temperature of 24.144°C, salinity of 22.180 PSU, and pH of 5.860, resulting in a predicted OD_{600} of 0.615 (Fig. 9D–F). To ensure experimental convenience, the strain was fermented at a temperature of 24°C, salinity of 22 PSU, and pH of 5.9 for 3 repeated experiments conducted over a period of 48 h each time. The average obtained OD_{600} value of 0.621 closely matched the value predicted by the model.

3.3.3. Strain G85

The OD_{600} values of strain G85 initially increased with the elevation in culture temperature, reaching a maximum value of 0.620 at 36°C, followed by a sharp decline to 0.047 at 44°C (Fig. 10A). The highest OD_{600} value of 0.564 was observed at 25 PSU, while the lowest value of 0.443 was recorded at 40 PSU (Fig. 10B). The effect of pH on strain G85 was similar to that on strain F65 (Fig. 10C). The regression model describing the relationship between the OD_{600} value of strain G85 and its growth-influencing factors is as follows:

$$OD_{600} = -18.92 + 0.71X_1 + 1.32X_2 + 1.62X_3 + 0.02X_1X_2 - 0.01X_1X_3 + 0.13X_2X_3 - 0.01X_1^2 - 0.59X_2^2 - 0.13X_3^2 \quad (4)$$

Based on model predictions, the optimal fermentation parameters were determined as follows: a culture temperature of 39.360°C, salinity of 23.440 PSU, and pH of 6.066, resulting in an expected OD_{600} value of 0.625 (Fig. 10D–F). For experimental convenience purposes, the strain was fermented at a temperature of 39°C, salinity of 23 PSU, and initial pH of 6.1 for 3 re-

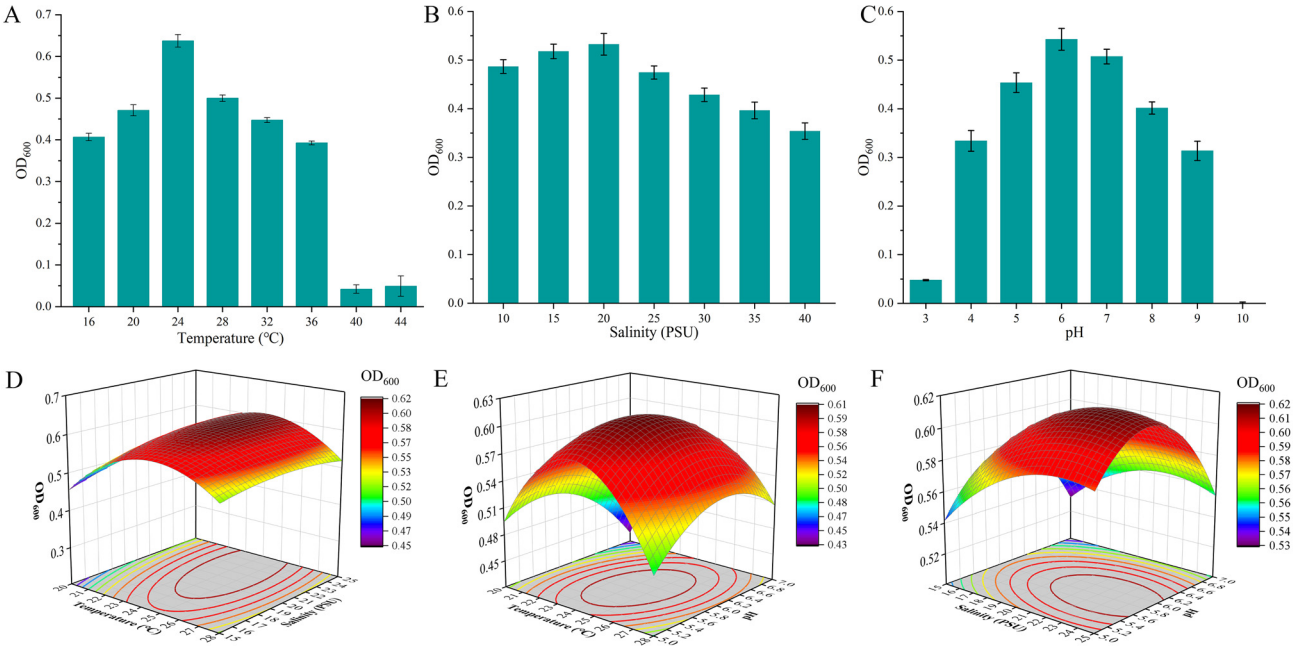

Fig. 9. As in Fig. 8, but for strain G84

peated experiments conducted over a period of 48 h each time. The average obtained OD_{600} value of 0.639 was approximately equal to that predicted by the model.

3.3.4. Strain G86

The OD_{600} of strain G86 initially increased with the elevation in culture temperature, reaching a maximum value of 0.620 at 28°C, followed by a decline to 0.050 at 44°C (Fig. 11A). The highest OD_{600} value of 0.615 was observed at 25 PSU, while the lowest value of 0.112 was observed at 40 PSU (Fig. 11B). Within the pH range of 3.0 to 7.0, the fermentation ability of strain G86 exhibited gradual improvement with increasing pH levels. At pH = 7.0, the strain displayed the highest fermentation capacity with an OD_{600} value of 0.601 (Fig. 11C). The regression model describing

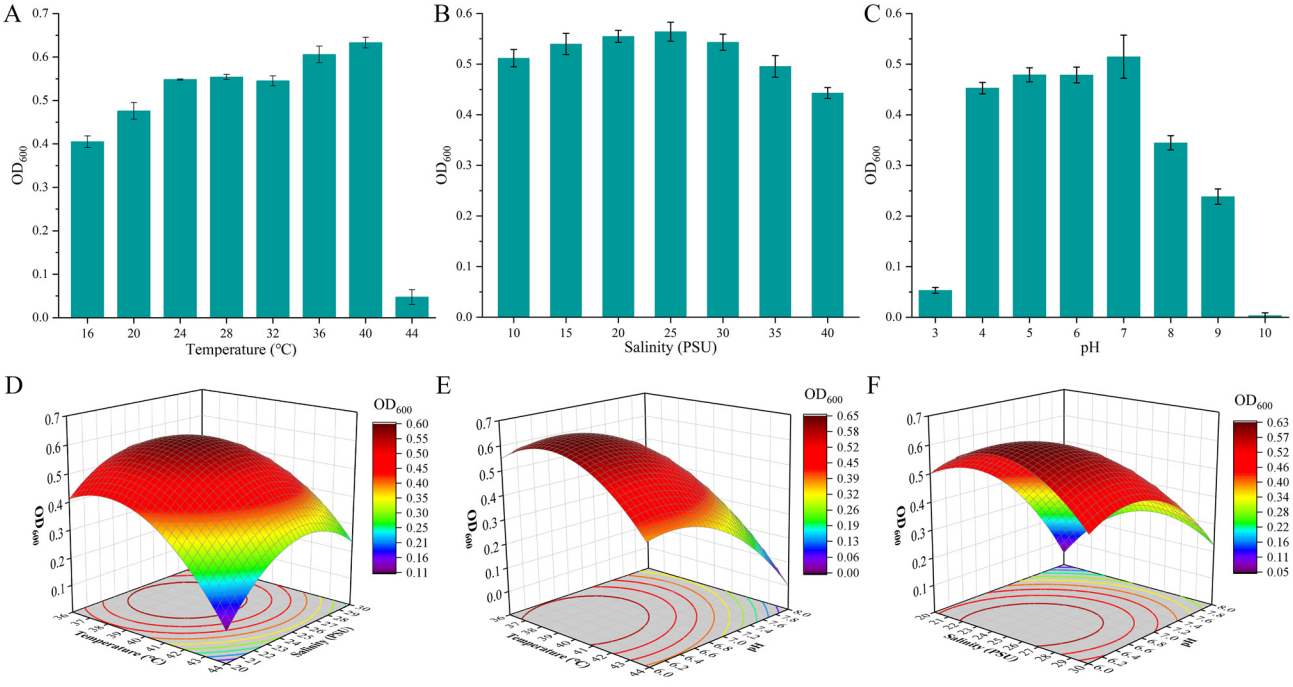

Fig. 10. As in Fig. 8, but for strain G85

the relationship between the OD_{600} value of strain G86 and the factors influencing its growth is as follows:

$$OD_{600} = -16.97 + 0.41X_1 + 2.33X_2 + 2.75X_3 - 0.03X_1X_2 - 0.01X_1X_3 + 0.01X_2X_3 - 0.01X_1^2 - 0.33X_2^2 - 0.20X_3^2 \quad (5)$$

Based on model predictions, the optimal fermentation parameters were determined to be a culture temperature of 26.928°C, salinity of 22.650 PSU, and pH of 6.858, resulting in a predicted OD_{600} value of 0.632 (Fig. 11D–F). For experimental convenience purposes, the strain was fermented at a temperature of 27°C, salinity of 23 PSU, and initial pH of 6.9 for 3 repeated experiments conducted over a period of 48 h each time. The average obtained OD_{600} value of 0.646 was approximately equal to that predicted by the model.

3.3.5. Strain I109

The OD_{600} of strain I109 initially increased with the elevation in culture temperature, reaching a maximum value of 0.612 at 40°C, followed by a decline to 0.027 at 44°C (Fig. 12A). Salinity levels ranging from 10 to 40 PSU exhibited negligible impacts on the proliferation of the strain (Fig. 12B). The highest OD_{600} value of 0.556 was observed at 25 PSU, while the lowest value of 0.369 was recorded at 40 PSU. Strain I109 exhibited a preference for weakly acidic conditions, with the maximum value of 0.687 being achieved at pH = 4.0 (Fig. 12C). The regression model describing the relationship between the OD_{600} value of strain I109 and the factors influencing its growth is as follows:

$$OD_{600} = -22.33 + 0.81X_1 + 1.86X_2 + 2.23X_3 + 0.02X_1X_2 - 0.02X_1X_3 - 0.01X_2X_3 - 0.01X_1^2 - 0.50X_2^2 - 0.17X_3^2 \quad (6)$$

Based on model predictions, the optimal fermentation parameters were determined to be a culture temperature of 38.619°C, salinity of 24.950 PSU, and pH of 4.338, resulting in a predicted OD_{600} value of 0.657 (Fig. 12D–F). For experimental convenience purposes, the strain was fermented at a temperature of 39°C, salinity of 25 PSU, and initial pH of 4.3 for 3 repeated experiments conducted over a period of 48 h each time. The average obtained OD_{600} value of 0.657 was equal to that predicted by the model.

4. DISCUSSION

4.1. Plant growth-promoting properties of bacterial strains isolated from *Zostera marina* rhizospheres

The isolates in our study exhibited favorable traits as potential PGPR, demonstrating diverse mechanisms that suggest their ability to enhance growth in *Zostera marina*. One of these advantageous charac-

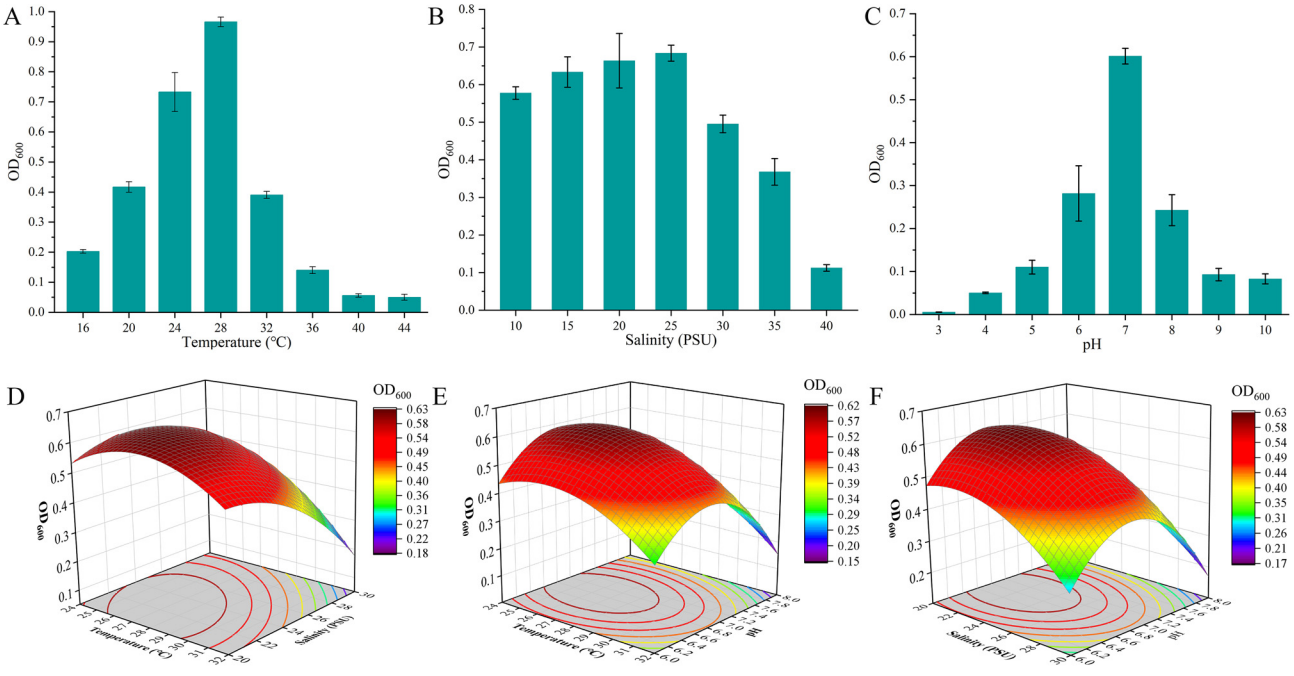

Fig. 11. As in Fig. 8, but for strain G86

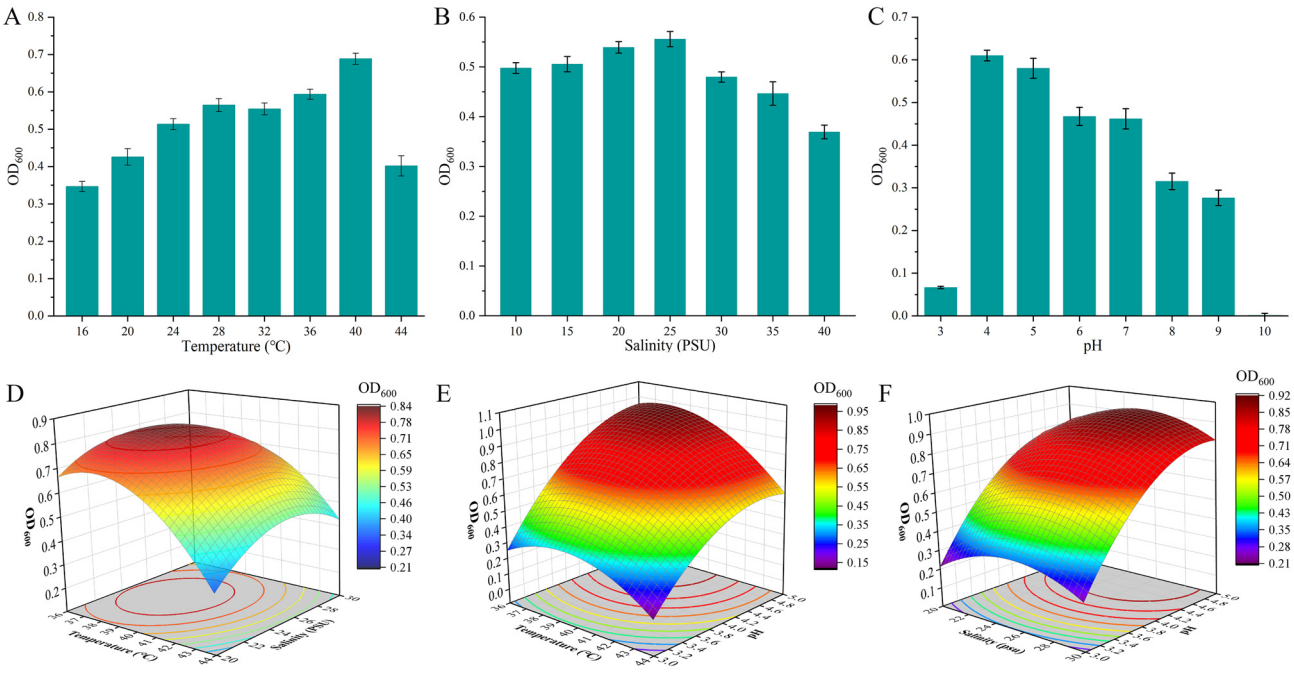

Fig. 12. As in Fig. 8, but for strain I109

teristics is evidenced by the presence of nitrogen-fixing genes within the bacterial strains. For instance, the isolated strains G84, G85, and G86 were able to thrive on a nitrogen-free medium. Seagrass growth, particularly, is often constrained by essential nutrient elements such as nitrogen and phosphorus (Touchette & Burkholder 2000). Specialized nitrogen-fixing bacteria play a crucial role in converting atmospheric nitrogen, which is not directly assimilable by most plants, into an organic form that can be accessed by plants (Nosheen et al. 2021). Recent studies have highlighted the essential contribution of nitrogen-fixing bacteria in fulfilling the nitrogen requirements of seagrasses (Mohr et al. 2021). Notably, rhizome-associated microorganisms have been identified as major suppliers, accounting for 65–90% of the necessary nitrogen for seagrass growth (Hansen et al. 2000, Cole & McGlathery 2012). In our study, heterotrophic diazotrophs were isolated from the rhizosphere of *Z. marina*, encompassing genera such as *Klebsiella*, *Shewanella*, *Pantoea*, *Novosphingobium*, and *Gallaecimonas*, most of which were identified as nitrogen-fixing strains (Merbach et al. 1997, Smit et al. 2012, He et al. 2021). Notably, *Pantoea* has also been isolated from *Thalassia hemprichii* (Ling et al. 2010), suggesting its potential ubiquity in both temperate and tropical seagrass ecosystems where it may exert a significant influence on nitrogen fixation.

The ability to solubilize rock phosphate is a promising trait for selecting bacteria capable of enhancing available phosphorus in the rhizosphere (Richardson & Simpson 2011, Bhattacharyya & Jha 2012). The strains isolated in this study, which belong to the common phosphorus-solubilizing *Pseudomonadota*, exhibited a range of phosphorus-soluble content from 14.6 to 393.9 mg l^{-1}. The variation in phosphate-solubilization abilities among bacterial strains can be attributed to factors such as genetic variation, environmental adaptations, and growth stages (Rawat et al. 2021). Acid secretion is a crucial mechanism employed by phosphate-solubilizing bacteria to dissolve insoluble phosphorus in soil (Rawat et al. 2021). In our experiment, the ability of strains to solubilize calcium phosphate exhibited a significant correlation with the reduction in pH of the culture medium, which can be attributed to the bacterial production of organic acids. The insoluble inorganic phosphorus can be effectively dissolved and released, thereby meeting the essential phosphorus requirements for seagrass growth. Assessing the ability of a strain for phosphorus dissolution through halo-based techniques often faces skepticism due to the possibility that certain isolates may not generate visible halos or bands on agar plates, yet they can effectively solubilize various forms of insoluble inorganic phosphates when cultivated in liquid media (Gupta et al. 1994). Similarly, our experiments also showed that PSI does not necessarily correspond to the ability of a strain to solubilize phosphorus. Some strains, such as F65 and J120, demonstrated substantial phosphate-solubilization capability despite lacking visible halos on Pikovskaya's agar, as revealed by quantitative experiments. There-

fore, future analogous studies should employ a more effective approach by integrating the halo method with other methodologies, such as the antimony–molybdenum colorimetric method.

Plant hormones play crucial roles in regulating various aspects of plant growth and development. Among these hormones, IAA has been widely studied as a kind of auxin, which controls processes such as cell division, elongation, differentiation, and pattern formation (Fu et al. 2015). For example, Li et al. (2024) demonstrated that monthly supplementation with 200 mg l^{-1} IAA effectively enhanced the leaf elongation rate, root vitality, and photosynthetic capacity of transplanted *T. hemprichii*. In addition to higher plants, the synthesis of IAA has also been observed in bacteria (Forni et al. 2017). Etesami et al. (2014) isolated and cultured 70 strains from the rhizosphere of rapeseed that produced IAA, and in pot experiments, all of the strains demonstrated superior colonization and growth-promoting activity on rice seedlings. Similarly, in our study, we identified 11 strains capable of producing IAA at concentrations ranging from 16.3 to 34.9 mg l^{-1}, highlighting their significant potential as PGPR.

Bacteria isolated from soil often possess the ability to produce siderophores, which play a crucial role in maintaining the iron cycle and promoting biodiversity and plant growth within the ecosystem (Timofeeva et al. 2022). For instance, Singh et al. (2020) found that 78% of strains isolated from rhizospheres demonstrated siderophore production, while do Carmo et al. (2011) observed this ability in 84% of bacteria from mangrove rhizospheres. In bacteria isolated from tropical seagrass, Lin et al. (2021) found that 44% exhibited siderophore production. In our experiments, approximately 73% of rhizosphere bacteria demonstrated the ability to produce siderophores.

4.2. Optimization of strain culture conditions

The impact of temperature on strain growth has been extensively investigated in previous studies (Rousk & Baath 2011, Patni et al. 2018). Our findings demonstrated that strains F65, G85, and I109 exhibited robust growth at approximately 40°C, while G84 and G86 thrived at around 24°C. The sensitivity of different strains to temperature varies (Diao et al. 2018, Wu et al. 2019). In general, extreme temperatures are detrimental to strain growth. Low temperatures tend to constrain cellular activity and metabolism (Berry & Foegeding 1997), whereas elevated temperatures can disrupt bacterial membrane structure, enzymes, DNA, and proteins, leading to a loss of vitality (Biran et al. 2018). In our study, we observed that when the ambient temperature reached 44°C, the growth of the tested strains was inhibited or stagnated.

The investigation of salt-tolerant microorganisms in agriculture has garnered significant attention (Etesami & Beattie 2018). For instance, Tiwari et al. (2011) successfully isolated salt-tolerant PGPR strains capable of withstanding NaCl concentrations ranging from 20 to 250 PSU, including bacteria such as *Pseudomonas mendocina*, *Bacillus pumilus*, *Halomonas* sp., and *Nitrinicola lacisaponensis*. In our study, strains F65, G84, G85, G86, and I109 exhibited remarkable adaptation to low-salinity conditions (10–40 PSU), displaying minimal growth and reproductive alterations in response to changes in salinity levels. These findings are consistent with previous studies (Larsen 1986, Etesami & Beattie 2018). However, the optimal growth range for these bacteria was observed at salinities of 20–25 PSU. This observation aligns well with the sedimentary conditions during strain screening within *Z. marina*.

The proliferation and energy metabolism of microbes are significantly influenced by environmental pH (Wang et al. 2011). In our study, strains F65, G84, G85, and I109 exhibited enhanced growth in neutral to weakly acidic environments, contrary to previous studies indicating their preference for neutral pH conditions (Nojoumi et al. 1995, Jung et al. 2002, Tantasuttikul & Mahakarnchanakul 2019). These variations can be attributed to the diverse growth requirements of different strains, even within the same genus, influenced by distinct isolation conditions (Sjöström & Larsson 1996, Bessa et al. 2012). Notably, these strains were isolated from the rhizosphere of *Z. marina*, which is rich in various small-molecule organic acids (Liu et al. 2014, Sun et al. 2021). Their ability to thrive in mildly acidic conditions enables colonization and growth within the *Z. marina* rhizosphere as demonstrated in previous studies (Zhalnina et al. 2018).

4.3. Conclusion

In summary, this study successfully isolated and characterized 45 strains from the rhizosphere of *Z. marina*. Among them, 5 strains (F65, G84, G85, G86, and I109) exhibited multiple growth-promoting properties including nitrogen fixation, phosphate solubilization, IAA production, siderophore production, and ammonia production. Notably, these strains also demonstrated remarkable adaptability to a wide range

of environmental conditions encompassing temperature variations as well as salinity and pH fluctuations. These findings underscore their potential as effective inoculants for providing essential nutrients to transplanted plants while promoting their growth and development. Subsequent mesocosm experiments and field trials are essential to elucidate the actual capabilities and mechanisms underlying the promotion effects of these strains on *Z. marina*.

Data availability. Data will be made available on request to the corresponding author

Acknowledgements. We thank Tian-Yu Wang, Yi Zhao, Xue-Jie Wang, and Ying-Song Wang for their assistance in sample collection, and Shun-Jie Yuan and Jin-Ji Liu for their assistance with sample collection and calculations. This study was supported by funds from the National Key Research and Development Program of China (2023YFD 2401102), the National Natural Science Foundation of China (42076100), Joint Funds of the National Natural Science Foundation of China (U2006214), and the Joint Research Center for Conservation, Restoration & Sustainable Utilization of Marine Ecology of Ocean University of China—China State Shipbuilding Corporation Environmental Development Co., Ltd. (H20240008).

LITERATURE CITED

Altschul SF, Gish W, Miller W, Myers EW, Lipman DJ (1990) Basic local alignment search tool. J Mol Biol 215:403–410

Bender SF, Wagg C, van der Heijden MGA (2016) An underground revolution: biodiversity and soil ecological engineering for agricultural sustainability. Trends Ecol Evol 31(6):440-452

Berry ED, Foegeding PM (1997) Cold temperature adaptation and growth of microorganisms. J Food Prot 60: 1583–1594

Bessa LJ, Correia DM, Cellini L, Azevedo NF, Rocha I (2012) Optimization of culture conditions to improve *Helicobacter pylori* growth in Ham's F-12 medium by response surface methodology. Int J Immunopathol Pharmacol 25: 901–909

Bhattacharyya PN, Jha DK (2012) Plant growth-promoting rhizobacteria (PGPR): emergence in agriculture. World J Microbiol Biotechnol 28:1327–1350

Biran D, Rotem O, Rosen R, Ron EZ (2018) Coping with high temperature: a unique regulation in *A. tumefaciens*. In: Gelvin SB (ed) *Agrobacterium* biology: from basic science to biotechnology. Springer, New York, NY, p 185–194

Bric JM, Bostock RM, Silverstone SE (1991) Rapid in situ assay for indoleacetic acid production by bacteria immobilized on a nitrocellulose membrane. Appl Environ Microbiol 57:535–538

Celdrán D, Espinosa E, Sánchez-Amat A, Marín A (2012) Effects of epibiotic bacteria on leaf growth and epiphytes of the seagrass *Posidonia oceanica*. Mar Ecol Prog Ser 456:21–27

Cole LW, McGlathery KJ (2012) Nitrogen fixation in restored eelgrass meadows. Mar Ecol Prog Ser 448:235–246

Diao H, Li L, Liang J, Ding X (2018) Screening of high-performance flocculant-producing bacteria and optimization of the conditions for flocculation of wheat distillery wastewater. BioResources 13:7738–7757

do Carmo FL, dos Santos HF, Martins EF, van Elsas JD, Rosado AS, Peixoto RS (2011) Bacterial structure and characterization of plant growth promoting and oil degrading bacteria from the rhizospheres of mangrove plants. J Microbiol 49:535–543

Duarte CM, Chiscano CL (1999) Seagrass biomass and production: a reassessment. Aquat Bot 65:159–174

Duarte CM, Marbà N, Gacia E, Fourqurean JW, Beggins J, Barrón C, Apostolaki ET (2010) Seagrass community metabolism: assessing the carbon sink capacity of seagrass meadows. Glob Biogeochem Cycles 24:GB4032

Dunic JC, Brown CJ, Connolly RM, Turschwell MP, Côté IM (2021) Long-term declines and recovery of meadow area across the world seagrass bioregions. Glob Change Biol 27:4096–4109

Etesami H, Beattie GA (2018) Mining halophytes for plant growth-promoting halotolerant bacteria to enhance the salinity tolerance of non-halophytic crops. Front Microbiol 9:148

Etesami H, Hosseini HM, Alikhani HA (2014) In planta selection of plant growth promoting endophytic bacteria for rice (*Oryza sativa* L.). J Soil Sci Plant Nutr 14:491–503

Forni C, Duca D, Glick BR (2017) Mechanisms of plant response to salt and drought stress and their alteration by rhizobacteria. Plant Soil 410:335–356

Fraser MW, Kendrick GA (2017) Belowground stressors and long-term seagrass declines in a historically degraded seagrass ecosystem after improved water quality. Sci Rep 7:14469

Fu SF, Wei JY, Chen HW, Liu YY, Lu HY, Chou JY (2015) Indole-3-acetic acid: a widespread physiological code in interactions of fungi with other organisms. Plant Signal Behav 10:e1048052

Gaby JC, Buckley DH (2012) A comprehensive evaluation of PCR primers to amplify the *nif*H gene of nitrogenase. PLOS ONE 7:e42149

Gupta R, Singal R, Skankar A, Kuhad RC, Saxena RK (1994) A modified plate assay for screening phosphate solubilizing microorganisms. J Gen Appl Microbiol 40:255–260

Hansen JW, Udy JW, Perry CJ, Dennison WC, Lomstein BA (2000) Effect of the seagrass *Zostera capricorni* on sediment microbial processes. Mar Ecol Prog Ser 199:83–96

Harborne AR, Mumby PJ, Micheli F, Perry CT, Dahlgren CP, Holmes KE, Brumbaugh DR (2006) The functional value of Caribbean coral reef, seagrass and mangrove habitats to ecosystem processes. Adv Mar Biol 50:57–189

He L, Karlep L, Li Z (2021) The nitrogen-cycling network of bacterial symbionts in the sponge *Spheciospongia vesparium*. J Ocean Univ China 20:999–1012

Houida S, Yakkou L, Kaya LO, Bilen S and others (2022) Biopriming of maize seeds with plant growth-promoting bacteria isolated from the earthworm *Aporrectodea molleri*: effect on seed germination and seedling growth. Lett Appl Microbiol 75:61–69

James RK, Silva R, Van Tussenbroek BI, Escudero-Castillo M and others (2019) Maintaining tropical beaches with seagrass and algae: a promising alternative to engineering solutions. BioScience 69:136–142

Jiang M, Delgado-Baquerizo M, Yuan MM, Ding J, Yergeau E, Zhou J (2023) Home-based microbial solution to boost crop growth in low-fertility soil. New Phytol 239:752–765

Jung I, Park DH, Park K (2002) A study of the growth condition and solubilization of phosphate from hydroxyapa-

tite by *Pantoea agglomerans*. Biotechnol Bioprocess Eng 7:201–205

Kloepper JW, Schroth MN (1978) Plant growth promoting rhizobacteria on radishes. In: Proceedings of the 4th International Conference on Plant Pathogenic Bacteria, Gibert-Clarey Imprimeurs, Tours, p 879–882

Lamb JB, Van De Water JA, Bourne DG, Altier C and others (2017) Seagrass ecosystems reduce exposure to bacterial pathogens of humans, fishes, and invertebrates. Science 355:731–733

Larsen H (1986) Halophilic and halotolerant microorganisms — an overview and historical perspective. FEMS Microbiol Rev 39:3–7

Leblanc ML, O'Connor MI, Kuzyk ZZA, Noisette F and others (2023) Limited recovery following a massive seagrass decline in subarctic eastern Canada. Glob Change Biol 29:432–450

Li Y, Zhang J, Zhang J, Xu W, Mou Z (2019) Characteristics of inorganic phosphate-solubilizing bacteria from the sediments of a eutrophic lake. Int J Environ Res Public Health 16:2141

Li Z, Shi Y, Zhao M, Shi Z, Luo H, Cai J, Han Q (2024) Plant growth regulators improve the growth and physiology of transplanted *Thalassia hemprichii* fragments. Front Mar Sci 11:1334937

Lin X, Dong J, Zhou W, Peng Q and others (2021) Isolation and diversity of plant growth-promoting bacteria on seagrass in Xincun Bay, Hainan. Yingyong Haiyangxue Xuebao (J Appl Oceanogr) 40:200–207

Ling J, Dong J, Zhang Y, Cai C, Wang Y, Zhang S (2010) Isolation and characterization of a N_2-fixing bacterium from coral reef-seagrass ecosystem. Microbiology 37: 962–968

Liu Y, Zhang N, Qiu M, Feng H, Vivanco JM, Shen Q, Zhang R (2014) Enhanced rhizosphere colonization of beneficial *Bacillus amyloliquefaciens* SQR9 by pathogen infection. FEMS Microbiol Lett 353:49–56

McKenzie LJ, Nordlund LM, Jones BL, Cullen-Unsworth LC, Roelfsema C, Unsworth RK (2020) The global distribution of seagrass meadows. Environ Res Lett 15:074041

Merbach W, Ruppel S, Schulze J (1997) Dinitrogen fixation of microbe–plant associations as affected by nitrate and ammonium supply. Isotopes Environ Health Stud 33:67–73

Milbrandt EC, Greenawalt-Boswell J, Sokoloff PD (2008) Short-term indicators of seagrass transplant stress in response to sediment bacterial community disruption. Bot Mar 51:103–111

Mohr W, Lehnen N, Ahmerkamp S, Marchant HK and others (2021) Terrestrial-type nitrogen-fixing symbiosis between seagrass and a marine bacterium. Nature 600:105–109

Moore KA (2009) Influence of seagrasses on water quality in shallow regions of the lower Chesapeake Bay. J Coast Res 45:162–178

Naamala J, Smith DL (2020) Relevance of plant growth promoting microorganisms and their derived compounds, in the face of climate change. Agronomy 10:1179

Nautiyal CS (1999) An efficient microbiological growth medium for screening phosphate solubilizing microorganisms. FEMS Microbiol Lett 170:265–270

Nojoumi SA, Smith DG, Rowbury RJ (1995) Tolerance to acid in pH 5.0-grown organisms of potentially pathogenic Gram-negative bacteria. Lett Appl Microbiol 21:359–363

Nosheen S, Ajmal I, Song YD (2021) Microbes as biofertilizers, a potential approach for sustainable crop production. Sustainability 13:1868

Orth RJ, Harwell MC, Fishman JR (1999) A rapid and simple method for transplanting eelgrass using single, unanchored shoots. Aquat Bot 64:77–85

Patni B, Panwar AS, Negi P, Joshi GK (2018) Plant growth promoting traits of psychrotolerant bacteria: a boon for agriculture in hilly terrains. Plant Sci Today 5:24–28

Rabbani G, Yan BC, Lee NLY, Ooi JLS, Lee JN, Huang D, Wainwright BJ (2021) Spatial and structural factors shape seagrass-associated bacterial communities in Singapore and Peninsular Malaysia. Front Mar Sci 8:659180

Rawat P, Das S, Shankhdhar D, Shankhdhar SC (2021) Phosphate-solubilizing microorganisms: mechanism and their role in phosphate solubilization and uptake. J Soil Sci Plant Nutr 21:49–68

Richardson AE, Simpson RJ (2011) Soil microorganisms mediating phosphorus availability. Plant Physiol 156: 989–996

Rousk J, Baath E (2011) Growth of saprotrophic fungi and bacteria in soil. FEMS Microbiol Ecol 78:17–30

Schwyn B, Neilands J (1987) Universal chemical assay for the detection and determination of siderophores. Anal Biochem 160:47–56

Serrano A, Mardad I, Soukri A (2013) Solubilization of inorganic phosphate and production of organic acids by bacteria isolated from a Moroccan mineral phosphate deposit. Afr J Microbiol Res 7:626–635

Short F, Carruthers T, Dennison W, Waycott M (2007) Global seagrass distribution and diversity: a bioregional model. J Exp Mar Biol Ecol 350:3–20

Singh RK, Singh P, Li HB, Guo DJ and others (2020) Plant–PGPR interaction study of plant growth-promoting diazotrophs *Kosakonia radicincitans* BA1 and *Stenotrophomonas maltophilia* COA2 to enhance growth and stress-related gene expression in *Saccharum* spp. J Plant Interact 15:427–445

Sjöström JE, Larsson H (1996) Factors affecting growth and antibiotic susceptibility of *Helicobacter pylori*: effect of pH and urea on the survival of a wild-type strain and a urease-deficient mutant. J Med Microbiol 44:425–433

Smit AM, Strabala TJ, Peng L, Rawson P, Lloyd-Jones G, Jordan TW (2012) Proteomic phenotyping of *Novosphingobium nitrogenifigens* reveals a robust capacity for simultaneous nitrogen fixation, polyhydroxyalkanoate production, and resistance to reactive oxygen species. Appl Environ Microbiol 78:4802–4815

Sun H, Jiang S, Jiang C, Wu C, Gao M, Wang Q (2021) A review of root exudates and rhizosphere microbiome for crop production. Environ Sci Pollut Res Int 28:54497–54510

Szitenberg A, Beca-Carretero P, Azcárate-García T, Yergaliyev T, Alexander-Shani R, Winters G (2022) Teasing apart the host-related, nutrient-related and temperature-related effects shaping the phenology and microbiome of the tropical seagrass *Halophila stipulacea*. Environ Microbiome 17:18

Tan YM, Dalby O, Kendrick GA, Statton J and others (2020) Seagrass restoration is possible: insights and lessons from Australia and New Zealand. Front Mar Sci 7:617

Tantasuttikul A, Mahakarnchanakul W (2019) Growth parameters and sanitizer resistance of *Raoultella ornithinolytica* and *Raoultella terrigena* isolated from seafood processing plant. Cogent Food Agric 5(1):1569830

Timofeeva AM, Galyamova MR, Sedykh SE (2022) Bacterial siderophores: classification, biosynthesis, perspectives of use in agriculture. Plants 11:3065

Tiwari S, Singh P, Tiwari R, Meena KK, Yandigeri M, Singh DP, Arora DK (2011) Salt-tolerant rhizobacteria-mediated

induced tolerance in wheat (*Triticum aestivum*) and chemical diversity in rhizosphere enhance plant growth. Biol Fertil Soils 47:907–916

Touchette BW, Burkholder JM (2000) Review of nitrogen and phosphorus metabolism in seagrasses. J Exp Mar Biol Ecol 250:133–167

Unsworth RK, Nordlund LM, Cullen-Unsworth LC (2019) Seagrass meadows support global fisheries production. Conserv Lett 12:e12566

van Katwijk MM, Bos AR, De Jonge VN, Hanssen LSAM, Hermus DCR, De Jong DJ (2009) Guidelines for seagrass restoration: importance of habitat selection and donor population, spreading of risks, and ecosystem engineering effects. Mar Pollut Bull 58:179–188

van Katwijk MM, Thorhaug A, Marbà N, Orth RJ and others (2016) Global analysis of seagrass restoration: the importance of large-scale planting. J Appl Ecol 53:567–578

Vogel MA, Mason OU, Miller TE (2021) Composition of seagrass phyllosphere microbial communities suggests rapid environmental regulation of community structure. FEMS Microbiol Ecol 97:fiab013

Wakarera PW, Ojola P, Njeru EM (2022) Characterization and diversity of native *Azotobacter* spp. isolated from semi-arid agroecosystems of Eastern Kenya. Biol Lett 18:20210612

Wang FQ, Shen QY, Chen GJ, Du ZJ (2015) *Mariniphaga sediminis* sp. nov., isolated from coastal sediment. Int J Syst Evol Microbiol 65:2908–2912

Wang L, English MK, Tomas F, Mueller RS (2021) Recovery and community succession of the *Zostera marina* rhizobiome after transplantation. Appl Environ Microbiol 87: e02326-20

Wang Y, Fang X, Cheng Y, Zhang X (2011) Manipulation of pH shift to enhance the growth and antibiotic activity of *Xenorhabdus nematophila.* J Biomed Biotechnol 2011: 672369

Wu Z, Lan M, Gao X, Li M and others (2019) Screening of fermentation conditions for herbicidal activity of *Pantoea agglomerans* strain ZLSY20. J South Agricult 50: 1990–1997

Zhalnina K, Louie KB, Hao Z, Mansoori N and others (2018) Dynamic root exudate chemistry and microbial substrate preferences drive patterns in rhizosphere microbial community assembly. Nat Microbiol 3:470–480

Zhang PD, Zhang LY, Niu SN, Sun Y, Tian L (2014) Effect of light intensity on survival, growth, and photosynthetic pigment of young seedlings of eelgrass *Zostera marina* Linnaeus, 1753 (Alismatales: Zosteraceae). Mar Biol Res 10:745–754

Zhang YH, Li C, Zhao JS, Li WT, Zhang PD (2020) Seagrass resilience: where and how to collect donor plants for the ecological restoration of eelgrass *Zostera marina* in Rongcheng Bay, Shandong Peninsula, China. Ecol Eng 158:106029

Zhang YH, Wang HH, Li F, Sun J, Li WT, Zhang PD (2022) The combined effect of planting density and sediment fertilization on survival, growth and physiology of eelgrass *Zostera marina.* Mar Pollut Bull 184:114136

Zheng F, Qiu G, Fan H, Zhang W (2013) Diversity, distribution and conservation of Chinese seagrass species. Biomed Sci 21:517–526

Zhuang L, Li Y, Wang Z, Yu Y and others (2021) Synthetic community with six *Pseudomonas* strains screened from garlic rhizosphere microbiome promotes plant growth. Microb Biotechnol 14:488–502

Editorial responsibility: John N. Griffin, Swansea, UK
Reviewed by: 3 anonymous referees

Submitted: January 12, 2024
Accepted: August 9, 2024
Proofs received from author(s): September 18, 2024